AIP Advances

Auger recombination rates in dilute-As GaNAs semiconductor

Chee-Keong Tan and Nelson Tansu

Citation: AIP Advances **5**, 057135 (2015); doi: 10.1063/1.4921394
View online: http://dx.doi.org/10.1063/1.4921394
View Table of Contents: http://scitation.aip.org/content/aip/journal/adva/5/5?ver=pdfcov
Published by the AIP Publishing

Articles you may be interested in

First-principle natural band alignment of GaN / dilute-As GaNAs alloy
AIP Advances **5**, 017129 (2015); 10.1063/1.4906569

Auger recombination rates in nitrides from first principles
Appl. Phys. Lett. **94**, 191109 (2009); 10.1063/1.3133359

Neutral base recombination in InP/GaAsSb/InP double-heterostructure bipolar transistors: Suppression of Auger recombination in p + GaAsSb base layers
Appl. Phys. Lett. **86**, 253506 (2005); 10.1063/1.1949290

Theoretical study of Auger recombination in a GaInNAs 1.3 μ m quantum well laser structure
Appl. Phys. Lett. **84**, 1826 (2004); 10.1063/1.1664033

Unusual increase of the Auger recombination current in 1.3 μm GaInNAs quantum-well lasers under high pressure
Appl. Phys. Lett. **82**, 2335 (2003); 10.1063/1.1566468

All article content, except where otherwise noted, is licensed under a Creative Commons Attribution 3.0 Unported license. See: http://creativecommons.org/licenses/by/3.0/ Downloaded to IP: 207.172.231.174 On: Fri, 15 May 2015 13:51:44

AIP ADVANCES **5**, 057135 (2015)

Auger recombination rates in dilute-As GaNAs semiconductor

Chee-Keong Tan[a] and Nelson Tansu[b]
Center for Photonics and Nanoelectronics, Department of Electrical and Computer Engineering, Lehigh University, Bethlehem, PA 18015, USA

(Received 31 March 2015; accepted 7 May 2015; published online 15 May 2015)

The evaluation of Auger recombination process for dilute-As GaNAs alloy is presented. Our analysis indicates the suppression of interband Auger recombination mechanism in dilute-As GaNAs alloy in the green spectral regime. The interband Auger coefficient in dilute-As GaNAs alloy is shown as two orders of magnitude lower than that of its corresponding intraband Auger rate. Our results confirm that the second conduction band has a negligible effect on the interband Auger process in dilute-As GaNAs alloy due to the non-resonant condition of the process. Our findings show the importance of dilute-As GaNAs as an alternative visible material with low Auger recombination rates. © *2015 Author(s). All article content, except where otherwise noted, is licensed under a Creative Commons Attribution 3.0 Unported License.* [http://dx.doi.org/10.1063/1.4921394]

I. INTRODUCTION

III-nitride semiconductor alloys have achieved significant progress in the past decade,[1–13] in which the key advances in III-Nitride based light emitting diodes (LEDs) were recently awarded by Nobel Prize in Physics in 2014.[14] Despite the advances in the GaN-based LEDs, LEDs development is hindered by the efficiency-droop phenomena which results in significant reduction in internal quantum efficiency as the operating current density increases. Various reasons have been suggested to contribute to the causes of efficiency droop in the InGaN-based LEDs.[15–32] The origin of the efficiency droop phenomena in the InGaN LEDs is still inconclusive, but research in recent years increasingly focused on the carrier density related mechanisms such as carrier leakage[16,17] and Auger recombination[18–30] in III-nitrides.

Most recently, Iveland and co-workers revealed a linear correlation between the emitted Auger electron and droop current in the InGaN LED, suggesting the existence and important role of Auger processes in leading to the efficiency droop in LEDs.[29] In particular, the interband Auger recombination process has been suggested as a dominant mechanism leading to large Auger coefficient values in the InGaN alloy, which accounts for the efficiency droop phenomena in green LEDs.[23] Previous study indicated the fundamental difficulties in suppressing the interband Auger recombination,[23] until our identification of dilute-As GaNAs material as a possible material with negligible interband Auger process.[30]

Dilute-As GaNAs alloy was recently shown as an alternative GaN-based material in addition to InGaN alloy that would provide narrow band gap emission, in particular for addressing blue up to yellow emission spectral regime.[30] Our recent studies have also clarified the heterojunction band alignment for dilute-As GaNAs/GaN interface,[33] which will be useful for enabling heterostructure-based device implementation. The research on dilute-As GaNAs alloy is however still limited,[3,30,33–37] in particular no quantification of the Auger recombination coefficients for this alloy had been reported. Evaluating the Auger recombination process quantitatively and confirming

[a]Electronic mail: ckt209@lehigh.edu
[b]Electronic mail: tansu@lehigh.edu

 ©Author(s) 2015

All article content, except where otherwise noted, is licensed under a Creative Commons Attribution 3.0 Unported license. See: http://creativecommons.org/licenses/by/3.0/ Downloaded to IP: 207.172.231.174 On: Fri, 15 May 2015 13:51:44

the suppression of interband Auger recombination using the dilute-As GaNAs alloy are thus critical to advance the technology based on this alloy.

In this work, we present quantitative findings of the Auger recombination coefficients in dilute-As $GaN_{1-x}As_x$ alloy for As-content (x) ranging from 0% up to 12.5%. The band properties of dilute-As GaNAs alloys are presented. The Auger recombination coefficients between dilute-As GaNAs alloy and InGaN alloy taking into consideration of both interband and intraband Auger recombination processes are compared. Our findings confirmed the suppression of interband Auger recombination by using dilute-As GaNAs alloy. Lastly, the temperature dependency of the Auger coefficient for dilute-As GaNAs alloy is briefly discussed.

II. THEORY AND CALCULATIONS

For intraband Auger recombination process, the energy released from the recombination between an electron and a hole is transferred to another carrier resulting in excitation of the carrier into a higher-energy state, as illustrated in figure 1(a). For the interband Auger recombination process, the carrier receiving the energy is excited to the second conduction band instead of the higher-energy state in the first conduction band, as illustrated in figure 1(b). In both cases, non-radiative recombination processes occurred under the energy and momentum conservation conditions.

In the framework of perturbation theory, a general Auger recombination rate is given by the following relation:[38,39]

$$R_{Auger} = 2\frac{2\pi}{\hbar}\left(\frac{V}{8\pi^3}\right)^3 \int\int\int\int |M_{1,1',2,2'}|^2 P_{1,1',2,2'} x\delta(E_{sum})\, x\delta\left(\vec{k}_{sum}\right) d\vec{k}_1 d\vec{k}_{1'} d\vec{k}_2 d\vec{k}_{2'} \quad (1)$$

In equation (1), state 1 and 2 are for electrons in the first conduction band, state 1' is for a heavy hole in the valence band and state 2' is for an electron in the second upper conduction band respectively. E_{sum} and $\vec{k}_{sum}$ stand for $E_{1'} + E_{2'} - E_1 - E_2$ and $\vec{k}_{1'} + \vec{k}_{2'} - \vec{k}_1 - \vec{k}_2$ (k-selection rule) respectively. The probability factor $P_{1,1',2,2'}$ is the term that accounts for the occupation probabilities of the carriers and $M_{1,1',2,2'}$ is the Auger matrix element. The equation (1) that involves computationally expensive twelvefold integrations of the momentum vector can be eased with analytical solution. The Auger coefficient (C), defined as $C = R/n^3$, is calculated using the analytical solutions in which the twelvefold integrations are simplified for carrier density up to $n \sim 10^{19}$ cm^{-3}.[38] Two specific analytical expressions for the Auger coefficients corresponding to the recombination process can be obtained for the cases of $E_g > \Delta$ and $E_g < \Delta$,[38] where E_g is the energy difference between the conduction band minimum of the first conduction band (CBM) and the valence band maximum (VBM) at the gamma point, and the parameter Δ is the energy difference between the CBM and

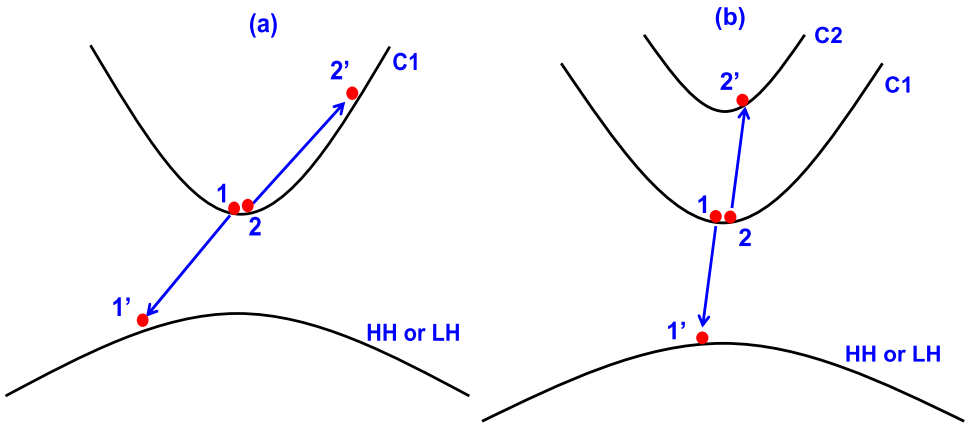

FIG. 1. Illustrations of (a) intraband Auger recombination process involving first conduction band (C1) and heavy hole (HH) or light hole (LH) band, and (b) interband Auger recombination process involving first conduction band (C1), second conduction band (C2) and heavy hole (HH) or light hole (LH) band.

All article content, except where otherwise noted, is licensed under a Creative Commons Attribution 3.0 Unported license. See: http://creativecommons.org/licenses/by/3.0/ Downloaded to IP: 207.172.231.174 On: Fri, 15 May 2015 13:51:44

TABLE I. Extracted band parameters from first-principle calculated band structures using LDA formalism for dilute-As GaNAs alloy from 0%-As up to 12.5%-As.[30]

$GaN_{1-x}As_x$	0%-As	1.56%-As	2.78%-As	6.25%-As	12.5%-As
E_g (eV)	3.645	3.325	3.109	2.376	2.232
Δ (eV)	2.246	2.091	2.107	1.783	1.663
m_e (m_0)	0.179	0.203	0.229	0.198	0.206
m_{hh} (m_0)	2.193	3.326	3.661	2.417	2.415
m_{lh} (m_0)	0.420	0.949	0.942	0.862	0.786
m_{c2} (m_0)	0.675	0.262	0.317	0.447	0.409

the conduction band minimum of the second conduction band. Table I provides the required band parameters of the dilute-As GaNAs alloys for the Auger coefficient calculations. The band parameters are extracted from the First-Principle calculated band structures of dilute-As GaNAs alloy, in which detailed computational descriptions for the band structure calculations can be found in our recent published work.[30]

III. RESULTS AND DISCUSSIONS

Note that the Auger calculation results from our models were compared with the experimental and other computational values obtained in InGaN and GaN alloys for validation purpose. Our calculated Auger coefficient for InGaN alloy was obtained as $C \sim 3.13 \times 10^{-30}$ cm^6s^{-1}, which agrees well with the experimental data ($C \sim 1.4\text{-}2.7 \times 10^{-30}$ cm^6s^{-1})[18–22] and with the theoretical results ($C \sim 2.0 \times 10^{-30}$ cm^6s^{-1}).[23,24] In addition, our calculated Auger coefficient for GaN alloy at T = 300K is $C = 2 \times 10^{-34}$ cm^6s^{-1}, which agrees considerably with the result by Bertazzi and co-workers.[25] The good agreements of our calculated Auger values for InGaN and GaN alloys with experimental results and computational works by others provide strong validation of the model used here.

Figure 2 shows the calculated Auger recombination coefficients of dilute-As $GaN_{1-x}As_x$ alloy with As-contents ranging from 0% up to 12.5%, which corresponds to active materials with emission wavelengths spanning from the ultraviolet up to the yellow spectral regime. The calculated Auger recombination coefficients of dilute-As GaNAs alloy take into account of both intraband and interband Auger recombination processes. The interband Auger recombination process includes the CHCC2 and CLCC2 Auger processes, while the intraband Auger recombination process includes CHCC and CLCC Auger processes. The CHCC2 (CLCC2) process denotes the Auger recombination process involving the C1 band, C2 band and HH (LH) band. In a similar context, the CHCC (CLCC) processes denote the Auger recombination process involving the C1 band and HH (LH) band.

As shown in figure 2, the calculated Auger recombination coefficients of dilute-As GaNAs alloys are compared to the reported Auger recombination coefficients of InGaN alloys.[23] As can be seen in figure 2, the reported Auger recombination coefficients for InGaN alloys constituted a "bell-shaped like" profile as a function of energy band gap value, which centered on the resonant condition of the interband Auger process in this alloy. The Auger recombination coefficient for InGaN alloy increases from 2×10^{-32} cm^6s^{-1} at 2.7 eV to 2×10^{-30} cm^6s^{-1} at 2.5 eV, then decreases from 2×10^{-30} cm^6s^{-1} at 2.5 eV to 1×10^{-31} cm^6s^{-1} at 2.3 eV. Note that without the influence of the interband Auger recombination process, the Auger recombination coefficients for InGaN alloy fall in the range of 1×10^{-34} cm^6s^{-1}, which is driven primarily by the intraband Auger process. The "bell-shape like" profile provides strong evidence of dominant interband Auger process in the material, which primarily resulted from the effect of the resonant energy condition ($E_g \approx \Delta$).[23]

Note that the interband Auger process is dominant at the ($E_g \approx \Delta$; also referred as on-resonant condition) as observed in InGaN material with bandgap of ~ 2.5 eV.[23] The resonant condition in the materials achieved for $E_g \approx \Delta$, which results in very large increase in the interband Auger

All article content, except where otherwise noted, is licensed under a Creative Commons Attribution 3.0 Unported license. See: http://creativecommons.org/licenses/by/3.0/ Downloaded to IP: 207.172.231.174 On: Fri, 15 May 2015 13:51:44

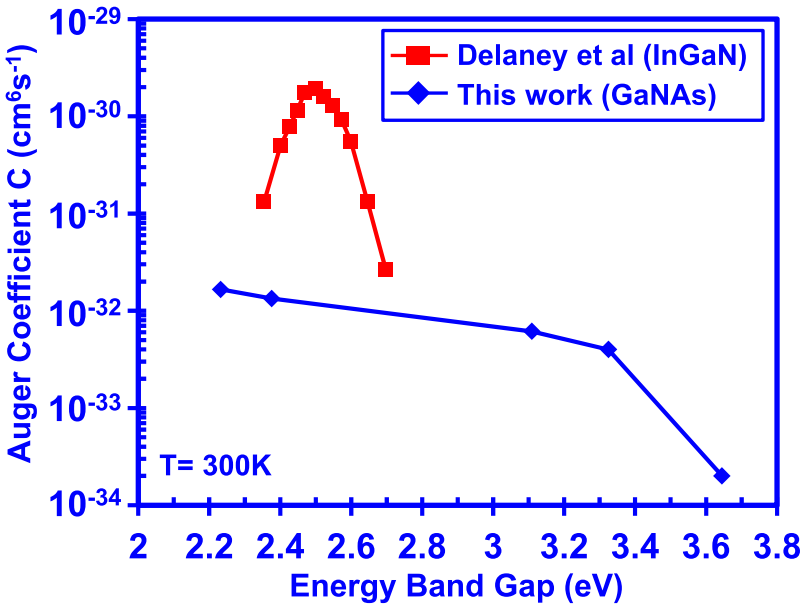

FIG. 2. The Auger coefficients for dilute-As GaNAs ternary alloy up to 12.5%-As considering interband and intraband Auger process at 300K. The calculated Auger coefficient results of dilute-As GaNAs alloy are compared to the reported Auger coefficients of InGaN alloy. The comparison results from Delaney and co-workers for InGaN were taken from Reference 23.

rate attributed to the simultaneous momentum and energy conservations with large carrier occupation probabilities. This condition was reported for InGaN material.[23] However, in our finding, the dilute-As GaNAs has E_g - $\Delta \sim 0.5$ eV, which results in non-resonant condition for the interband Auger process to be dominant.

The Auger recombination coefficients for dilute-As $GaN_{1-x}As_x$ alloy with x = 0% up to x = 12.5% is significantly suppressed over those of the InGaN alloy. The calculated Auger coefficient increases from 2 x 10^{-34} cm^6s^{-1} with 0% As-content of GaNAs alloy at 3.645 eV to 1.66 x 10^{-32} cm^6s^{-1} with 12.5% As-content of GaNAs alloy at 2.232 eV. The maximum Auger recombination coefficient of dilute-As GaNAs alloy is about two orders of magnitude smaller than that of InGaN alloy. In addition, the Auger recombination coefficients of dilute-As GaNAs alloy do not exhibit a bell-shaped profile like InGaN alloy, which can be readily understood from the negligible interband Auger process in this material. The low interband Auger rate in dilute-As GaNAs is attributed primarily to its large E_g-$\Delta > 0.5$ eV, resulting in non-resonant energy condition for such process to be dominant.[30]

Further analysis on the impact of interband Auger recombination in dilute-As GaNAs alloy is presented. Figure 3(a) shows a comparison between interband and intraband Auger recombination coefficients for dilute-As GaNAs alloys from 0%-As up to 12.5%-As at 300K. As presented in figure 3(a), the interband Auger recombination process yields a maximum Auger coefficient of 3.42 x 10^{-34} cm^6s^{-1} while the intraband Auger recombination process yields a maximum Auger coefficient of 1.62 x 10^{-32} cm^6s^{-1} in GaNAs alloy of 12.5%-As-content at T = 300K. Our finding strongly indicates that the interband Auger rates are at least two orders of magnitude smaller than the corresponding intraband Auger rates for dilute-As GaNAs alloy. The Auger rate in dilute-As GaNAs alloy is dominated by the intraband process, and this rate is approximately two orders of magnitude smaller than those predicted for InGaN alloy.

As previously elaborated,[23,30] the interband Auger process is shown to have exponential dependency to the parameter E_g-Δ for a particular semiconductor. The strong mismatch of E_g-Δ in dilute-As GaNAs results in off-resonance condition, which in turn leads to a significant reduction in the interband Auger rate in the alloy. The effect of the off-resonance condition (E_g-$\Delta \neq 0$) on the interband Auger rates in dilute-As GaNAs can be illustrated in the ratio of the relative comparison on the Auger rate plotted as function of the E_g-Δ, as shown in figure 3(b). Figure 3(b) shows that the

All article content, except where otherwise noted, is licensed under a Creative Commons Attribution 3.0 Unported license. See: http://creativecommons.org/licenses/by/3.0/ Downloaded to IP: 207.172.231.174 On: Fri, 15 May 2015 13:51:44

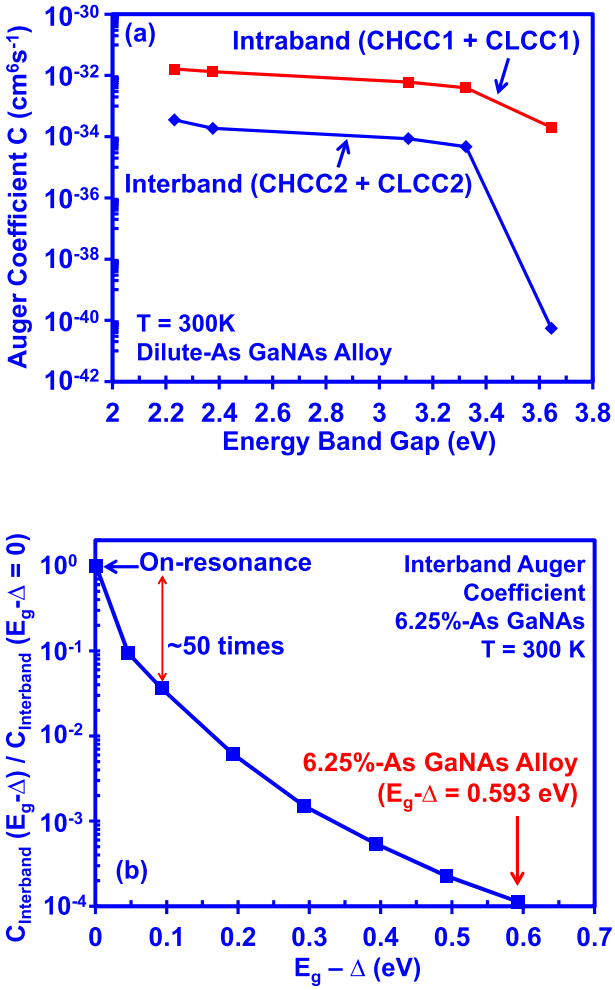

FIG. 3. (a) A comparison between interband and intraband Auger coefficient for dilute-As GaNAs ternary alloy up to 12.5%-As at 300K. Note that the interband Auger process consists of CHCC2 and CLCC2 transitions, and the intraband Auger process consists of CHCC1 and CLCC1 transitions. Figure 3(b) shows the effect of parameter E_g-Δ onto the interband Auger recombination rate.

interband Auger process will be significantly suppressed by at least two orders of magnitude attributed directly from the off-resonance condition (E_g-Δ > 100 meV). This implies the important role of the parameter E_g-Δ energy in the interband Auger recombination process, which also suggests the importance of having large E_g-Δ energy to suppress the interband Auger recombination process in a semiconductor alloy.

Figure 4(a) and 4(b) show the temperature dependency of the Auger recombination coefficients for dilute-As GaNAs ternary alloy from 1.56%-As up to 12.5%-As with a temperature range from 80K to 600K. The Auger coefficients (C) for dilute-As GaNAs alloys show an increasing trend for increasing temperature. Our findings show that the Auger coefficients for dilute-As GaNAs are in the range of $C \sim 10^{-31}$ cm^6s^{-1} for temperature T ~ 600 K, and the coefficients are in the range of 10^{-37} - 10^{-38} cm^6s^{-1} for T = 80 K. Specifically, the Auger recombination coefficient for 6.25%-As GaNAs alloy reaches 1.57 x 10^{-31} cm^6s^{-1} at T = 600K and decreases to only 8.36 x 10^{-39} cm^6s^{-1} at T = 80K.

The trends shown in figure 4(a) and 4(b) are expected for dilute-As GaNAs alloys. The higher temperature results in the Fermi-Dirac function broadening leading to an increase in occupation probability for the carriers, which in turn increases the Auger rate. The Auger rate is shown to have saturation at high temperature primarily limited by restriction from the momentum conservation

All article content, except where otherwise noted, is licensed under a Creative Commons Attribution 3.0 Unported license. See: http://creativecommons.org/licenses/by/3.0/ Downloaded to IP: 207.172.231.174 On: Fri, 15 May 2015 13:51:44

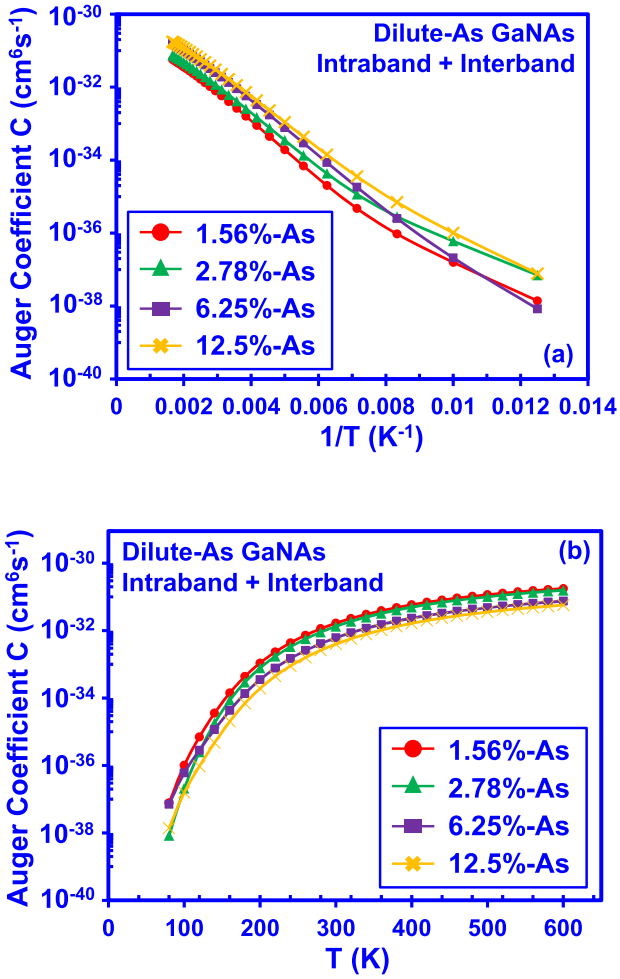

FIG. 4. Temperature dependency of Auger coefficients for dilute-As GaNAs ternary alloy from 1.56%-As up to 12.5%-As plotted as a function of (a) 1/ T and (b) T for a temperature range from T = 80 K up to T = 600 K.

rule. Note that in this study the effective mass and energy band gap of the dilute-As GaNAs alloys are assumed to be constant over the temperature range. Further studies are required to account for the high temperature characteristics of the Auger rate for dilute-As GaNAs by taking into consideration the temperature variation in its band parameters.

IV. CONCLUSIONS

In summary, the direct Auger recombination rate in the dilute-As GaNAs alloy from 0%-As up to 12.5%-As is quantitatively determined through the First-Principle approach. The maximum Auger recombination coefficient considering intraband and interband Auger recombination processes for dilute-As GaNAs alloy is found as $C \sim 1.66 \times 10^{-32}$ cm^6s^{-1}, which is two orders of magnitude lower than that of InGaN alloy. The interband Auger coefficient is also found to be at least two orders of magnitude smaller than its corresponding intraband Auger coefficient for dilute-As GaNAs alloy. The pursuits of experimental synthesis of dilute-As were initiated about two decades ago.[2,3] However, the lack of a clear motivating factor in the pursuit of dilute-As GaNAs beyond serving as another method to achieve visible light emission in III-Nitride system had resulted in relatively little progress in this area.[34–37] Our findings on the low Auger rate in dilute-As GaNAs provide a strong motivation for the pursuit of this material as a possible active material for visible LEDs and lasers operating at high operating current density.

All article content, except where otherwise noted, is licensed under a Creative Commons Attribution 3.0 Unported license. See: http://creativecommons.org/licenses/by/3.0/ Downloaded to IP: 207.172.231.174 On: Fri, 15 May 2015 13:51:44

ACKNOWLEDGMENTS

The work was supported by US National Science Foundation (ECCS 1408051, ECCS 1028490, DMR 1505122), and the Daniel E. ′39 and Patricia M. Smith Endowed Chair Professorship Fund. The authors also acknowledge helpful technical discussions with Dr. Hannes Schweiger from Material Design. The authors also would like to acknowledge useful discussions with Dr. Benjamin O. Tayo, Dr. Jing Zhang, and Dr. Guangyu Liu, all from Lehigh University.

[1] S. Nakamura, M. Senoh, N. Iwasa, and S. Nagahama, Appl. Phys. Lett. **67**, 1868-1870 (1995).
[2] X. Li, S. G. Bishop, and J. J. Coleman, Appl. Phys. Lett. **73**, 1179-1181 (1998).
[3] X. Li, S. Kim, E. E. Reuter, S. G. Bishop, and J. J. Coleman, Appl. Phys. Lett. **72**, 1990-1992 (1998).
[4] M. Krames, O. Shchekin, R. Mueller-Mach, G. Mueller, L. Zhou *et al.*, J. Disp. Technol. **3**, 160-175 (2007).
[5] I. H. Brown, P. Blood, P. M. Smowton, J. D. Thomson, S. M. Olaizola, A. M. Fox, P. J. Parbrook, and W. W. Chow, IEEE J. Quantum Electron. **42**, 1202-1208 (2006).
[6] M. H. Crawford, IEEE. J. Sel. Top. Quantum Electron. **15**, 1028-1040 (2009).
[7] M. Zhang, P. Bhattacharya, and W. Guo, Appl. Phys. Lett. **97**, 011103 (2010).
[8] H. Zhao, G. Y. Liu, J. Zhang, J. D. Poplawsky, V. Dierolf, and N. Tansu, Opt. Express **19**, A991-A1007 (2011).
[9] A. Laubsch, M Sabathil, J. Baur, M. Peter, and B. Hahn, IEEE Trans. Electron Devices **57**, 79-87 (2010).
[10] G. Y. Liu, J. Zhang, C. K. Tan, and N. Tansu, IEEE Photon. J. **5**, 2201011 (2013).
[11] J. Zhang and N. Tansu, IEEE Photon. J. **5**, 2600111 (2013).
[12] D. F. Feezell, J. S. Speck, S. P. DenBaars, and S. Nakamura, J. Display Tech. **9**, 190-198 (2013).
[13] J. Y. Tsao, M. H. Crawford, M. E. Coltrin, A. J. Fischer, D. D. Koleske, G. S. Subramania, G. T. Wang, J. J. Wierer, and R. F. Karlicek, Jr., **2**, 809-836 (2014).
[14] http://www.nobelprize.org/nobel_prizes/physics/laureates/2014/.
[15] J. Piprek, Phys. Status Solidi A **207**, 2217-2225 (2010).
[16] M. H. Kim, M. F. Schubert, Q. Dai, J. K. Kim, E. F. Schubert, J. Piprek, and Y. Park, Appl. Phys. Lett. **91**, 183507 (2007).
[17] H. P. Zhao, G. Y. Liu, J. Zhang, R. A. Arif, and N. Tansu, J. Display Technol. **9**, 212-225 (2013).
[18] Y. C. Shen, G. O. Mueller, S. Watanabe, N. F. Gardner, A. Munkholm, and M. R. Krames, Appl. Phys. Lett. **91**, 141101 (2007).
[19] P. G. Eliseev, M. Osin'ski, H. Li, and I. V. Akimova, Appl. Phys. Lett. **75**, 3838-3840 (1999).
[20] M. Zhang, P. Bhattacharya, J. Singh, and J. Hinckley, Appl. Phys. Lett. **95**, 201108 (2009).
[21] M. Meneghini, N. Trivellin, G. Meneghesso, and E. Zanoni, J. Appl. Phys. **106**, 114508 (2009).
[22] D. A. Zakheim, A. S. Pavluchenko, D. A. Bauman, K. A. Bulashevich, O. V. Khokhlev, and S. Y. Karpov, Phys. Status Solidi A **209**, 456-460 (2012).
[23] K. T. Delaney, P. Rinke, and C. G. Van de Walle, Appl. Phys. Lett. **94**, 191109 (2009).
[24] G. Hatakoshi and S. Nunoue, Jap. J. Appl. Phys. **52**, 08JG17 (2013).
[25] F. Bertazzi, M. Goano, and E. Bellotti, Appl. Phys. Lett. **97**, 231118 (2010).
[26] F. Bertazzi, X. Zhou, M. Goano, G. Ghione, and E. Bellotti, Appl. Phys. Lett. **103**, 081106 (2013).
[27] E. Kioupakis, P. Rinke, K. T. Delaney, and C. G. Van de Walle, Appl. Phys. Lett. **98**, 161107 (2011).
[28] A. David and M. J. Grundmann, Appl. Phys. Lett. **96**, 103504 (2010).
[29] J. Iveland, L. Martinelli, J. Peretti, J. S. Speck, and C. Weisbuch, Phys. Rev. Lett. **110**, 177406 (2013).
[30] C. K. Tan, J. Zhang, X. H. Li, G. Y. Liu, B. O. Tayo, and N. Tansu, J. Dis. Tech. **9**, 272-279 (2013).
[31] A. A. Efremov, N. I. Bochkareva, R. I. Gorbunov, D. A. Lavrinovich, Y. T. Rebane, D. V. Tarkhin, and Y. G. Shreter, Semiconductors **40**, 605-610 (2006).
[32] X. Guo and E. F. Schubert, J. Appl. Phys. **90**, 4191-4195 (2001).
[33] C. K. Tan and N. Tansu, AIP Adv. **5**, 017219 (2015).
[34] A. Kimura, C. A. Paulson, H. F. Tang, and T. F. Kuech, Appl. Phys. Lett. **84**, 1489-1491 (2004).
[35] R. A. Arif, H. Zhao, and N. Tansu, Appl. Phys. Lett. **92**, 011104 (2008).
[36] J. Wu, W Walukiewicz, K. M. Yu, J. D. Denlinger, W. Shan, J. W. Ager III, A. Kimura, H. F. tang, and T. F. Kuech, Phys. Rev. B **70**, 115214 (2004).
[37] K. M. Yu, S. V. Novikov, R. Broesler, C. R. Staddon, M. Hawkridge, Z. Liliental-Weber, I. Demchenko, J. D. Denlinger, V. M. Kao, F. Luckert, R. W. Martin, W. Walukiewicz, and C. T. Foxon, Phys. Status Solidi C **7**, 1847-1849 (2010).
[38] A. Haug, D. Kerkhoff, and W. Lochmann, Phys. Status Solidi B **89**, 357-365 (1978).
[39] D. B. Laks, G. F. Neumark, and S. T. Pantelides, Phys. Rev. B **42**, 5176-5185 (1990).

All article content, except where otherwise noted, is licensed under a Creative Commons Attribution 3.0 Unported license. See: http://creativecommons.org/licenses/by/3.0/ Downloaded to IP: 207.172.231.174 On: Fri, 15 May 2015 13:51:44